

# Gravitational Lensing of QSOs by Their Damped Ly $\alpha$ Absorbers

Matthias Bartelmann<sup>1,2</sup> and Abraham Loeb<sup>1</sup>

<sup>1</sup>Harvard-Smithsonian Center for Astrophysics, 60 Garden Street, Cambridge, MA 02138;

<sup>2</sup>Max-Planck-Institut für Astrophysik, Postfach 1523, D-85740 Garching, FRG

submitted to *The Astrophysical Journal*

*Abstract.* Damped Ly $\alpha$  absorbers are believed to be associated with galactic disks. We show that gravitational lensing can therefore affect the statistics of these systems. First, the magnification bias due to lensing raises faint QSOs above a given magnitude threshold and thereby enhances the probability for observing damped absorption systems. Second, the bending of light rays from the source effectively limits the minimum impact parameter of the line-of-sight relative to the center of the absorber, thus providing an upper cut-off to the observed neutral-hydrogen (HI) column density. The ray-bending also reduces a possible obscuration of the QSO by dust. The combination of the lensing effects yields a pronounced peak in the observed abundance of absorbers with high column densities ( $\gtrsim 2 \times 10^{21} \text{ cm}^{-2}$ ) and low redshifts ( $z_{\text{abs}} \lesssim 1$ ) in the spectra of bright QSOs ( $B \lesssim 18 \text{ mag}$ ) with redshifts  $z_{\text{QSO}} \gtrsim 2$ . The inferred value of the cosmological density parameter of neutral hydrogen,  $\Omega_{\text{HI}}$ , increases with increasing redshift and luminosity of the sources even if the true HI density remains constant. This trend resembles the observed evolution of  $\Omega_{\text{HI}}(z)$ . Damped Ly $\alpha$  absorbers with column densities  $\gtrsim 10^{21} \text{ cm}^{-2}$  and redshifts  $0.5 \lesssim z_{\text{abs}} \lesssim 1$  are reliable flags for lensed QSOs with a close pair of images separated by  $\sim 0.3''$  ( $v_c/220 \text{ km s}^{-1}$ )<sup>2</sup>, where  $v_c$  is the rotational velocity of the lens. Detection of these gravitational-lensing signatures with the *Hubble Space Telescope* can be used to constrain the depth of the absorber potential-wells and the cosmological constant.

*Key words:* Cosmology: Gravitational Lensing — Cosmology: Large-Scale Structure of Universe — Galaxies: Evolution — Quasars: Absorption Lines

## 1. Introduction

Most of the neutral hydrogen probed by QSO absorption spectra is traced by damped Ly $\alpha$  absorption lines, corresponding to HI column densities of  $10^{20-22} \text{ cm}^{-2}$  (see, e.g. Wolfe 1988; Lanzetta, Wolfe, & Turnshek 1995). The high HI content and the cosmological

abundance of damped Ly $\alpha$  systems suggest that they are associated with galactic disks (Wolfe 1988). Direct evidence for this identification is indeed provided by a wealth of observational facts. First, recent images of QSOs exhibiting damped Ly $\alpha$  systems in their spectra show related galaxies (cf. Steidel et al. 1994, 1995). Second, abundant heavy-element absorption lines at low ionization stages are frequently associated with damped Ly $\alpha$  absorption systems (Turnshek et al. 1989; Wolfe et al. 1993; Pettini et al. 1994). Third, the velocity field traced by these metal lines relative to the damped Ly $\alpha$  line is consistent with typical galactic rotation velocities, if the damped component is associated with a galactic disk while the metal-line systems are embedded in a surrounding halo (Lanzetta & Bowen 1992; Lu et al. 1993; Turnshek & Bohlin 1993; Lu & Wolfe 1994). Fourth, observations of redshifted 21-cm absorption and emission indicate disk-like structures that extend across galactic dimensions (Briggs et al. 1989; Wolfe et al. 1992). Fifth, Faraday-rotation observations of QSOs with damped Ly $\alpha$  systems are consistent with the existence of micro-Gauss magnetic fields in the absorbers, of the same magnitude as detected in nearby disk galaxies (Welter, Perry, & Kronberg 1984; Wolfe, Lanzetta, & Oren 1992; Perry, Watson, & Kronberg 1993; however note the caveat in Kronberg, Perry, & Zukowski 1992). Based on these clues, we adopt the view that damped Ly $\alpha$  absorption arises from neutral hydrogen in ordinary disk galaxies.

The characteristic HI density profiles of nearby spiral galaxies can be used to get a rough estimate of the impact parameter of lines-of-sight to QSOs relative to the centers of damped Ly $\alpha$  absorbers. Typical HI column densities of  $\gtrsim 2 \times 10^{20} \text{ cm}^{-2}$  imply impact parameters  $\lesssim 15 h^{-1} \text{ kpc}$  (Broeils & van Woerden 1994). This characteristic separation is indeed confirmed by direct imaging (Steidel et al. 1994, 1995). Geometrically, the absorbing disk can be intersected through a variety of impact parameters, with some lines of sight passing very close to the center of the absorber. If the damped systems resemble nearby disk galaxies, then the effects of gravitational lensing are strong and inevitable for lines-of-sight passing less than a few kpc from the absorber center, where the HI column density is high. The statistics of high column-density systems would then be marked by a pronounced lensing signature.

Gravitational lensing gives rise to two distinct effects. First, it magnifies the flux of the background QSO population and thus increases the number of sources above a given magnitude limit (see, e.g., Narayan & Wallington 1993; Schneider, Ehlers, & Falco 1992; Schneider 1992). The magnification bias tends to artificially increase the fraction of QSOs which show damped Ly $\alpha$  systems. Second, the bending of light rays effectively limits the minimum impact parameter of the line-of-sight towards the QSO relative to the absorber center, and therefore provides an upper cut-off to the column-density distribution of damped Ly $\alpha$  absorbers. The strength of these lensing effects depends on the depth of the gravitational potential-well of the absorbers, and on the underlying cosmology. Within the framework of Friedmann-Lemaître cosmological models, a possible non-zero cosmological constant has a strong influence on the statistics of lensing events (Turner 1990; Kochanek 1992).

The magnification bias is most pronounced for high column-density absorbers in the spectra of bright QSOs. Systems specified by these two requirements are particularly easy to observe, given a sufficiently large sample of QSOs. The search for the lensing signature

requires space-based observations because lensing is primarily effective for absorbers at redshifts  $z_{\text{abs}} \sim 0.5\text{--}1$  and sources at  $z_{\text{QSO}} \gtrsim 2$ . Unfortunately, existing surveys of damped Ly $\alpha$  systems using ground-based and *IUE* observations (see, e.g., Lanzetta et al. 1995, and references therein) do not cover simultaneously the redshift ranges for absorbers and sources which are optimal for lensing. However, it should be straightforward to extend these surveys and to design an optimal search strategy that will probe the lensing signatures predicted in this paper through future observations with the *Hubble Space Telescope*. If gravitational lensing indeed occurs in damped Ly $\alpha$  absorption systems, one would expect the formation of multiple QSO images especially in high column-density systems. It is, however, not surprising that multiple images were not resolved in such systems in the past, because the characteristic image splitting provided by spiral galaxies is  $\lesssim 0.3''$ . Damped Ly $\alpha$  absorption at a fairly low column density,  $\sim 7 \times 10^{19} \text{ cm}^{-2}$ , was observed in the spectrum of both images of QSO 0957 + 561 (Turnshek & Bohlin 1993), but in that case the large angular separation of  $\sim 6''$  is caused by an intervening galaxy cluster.

The magnification bias also affects estimates for the value of the cosmological density parameter of neutral hydrogen in damped Ly $\alpha$  systems,  $\Omega_{\text{HI}}$ . It has recently been argued that the observed decline of  $\Omega_{\text{HI}}$  between  $z \sim 3.5$  and the present time (White, Kinney, & Becker 1993; Bahcall et al. 1993; Lanzetta et al. 1995) is a natural consequence of the conversion of gas into stars in disk galaxies (Kauffmann & Charlot 1994; Lanzetta et al. 1995). Here, we examine the effect of lensing on the estimate of  $\Omega_{\text{HI}}(z)$ . Although high column-density systems are rare their contribution to the estimate of  $\Omega_{\text{HI}}$  is dominant, and so the lensing effect on their apparent abundance can change the apparent value of  $\Omega_{\text{HI}}$  considerably. In particular, we show that the inferred value of  $\Omega_{\text{HI}}$  should generically decline with decreasing source redshift even if the true HI density in the absorbers remains constant. This apparent evolution results from the change in the efficiency of lensing with redshift.

Thomas & Webster (1990) used a simplified model to examine the influence of the magnification bias on the observed statistics of metal absorption lines in QSO spectra. They concluded that the redshift distribution of the absorbers is at most weakly affected by lensing. Our study focuses on damped Ly $\alpha$  absorption systems which are more likely to arise at small impact parameters where lensing is expected to be stronger. Moreover, we address additional statistical properties of the absorbers which are more sensitive to gravitational lensing.

The outline of this paper is as follows. In §2 we develop the formalism required to investigate the various signatures of gravitational lensing. We adopt the simplest model for damped Ly $\alpha$  absorbers, assuming no cosmological evolution in their HI density profiles, which we model according to observed profiles in nearby disk galaxies. This simple model provides a good fit to the observed column-density distribution of the damped Ly $\alpha$  systems. Moreover, the strongest lensing signature is expected for absorbers at low redshift ( $z_{\text{abs}} \sim 0.5$ ), where evolutionary effects due to mergers or accretion should be weak (Tóth & Ostriker 1992; Zaritsky 1995). The numerical results for the various lensing signatures are presented in §3. Finally, §4 summarizes our main conclusions.

## 2. Formalism

### 2.1. Parameterization of the Absorber Population

In the following subsections, we calculate the probability that intervening disk galaxies produce damped Ly $\alpha$  absorption and simultaneously magnify the background QSOs whose spectra show the absorption lines. We assume that the absorber population can be parameterized by the Schechter luminosity function (Schechter 1976),

$$\Phi(\ell) d\ell = \Phi_* \ell^s \exp(-\ell) d\ell, \quad (2.1)$$

where  $\ell \equiv (L/L_*)$  is the luminosity in units of the luminosity scale  $L_*$ , and where, for spiral galaxies (Marzke et al. 1994)

$$\Phi_* = 1.5 \times 10^{-2} h^3 \text{ Mpc}^{-3}, \quad s = -0.81. \quad (2.2)$$

As usual,  $h$  is the Hubble constant  $H_0$  in units of  $100 \text{ km s}^{-1} \text{ Mpc}^{-1}$ .

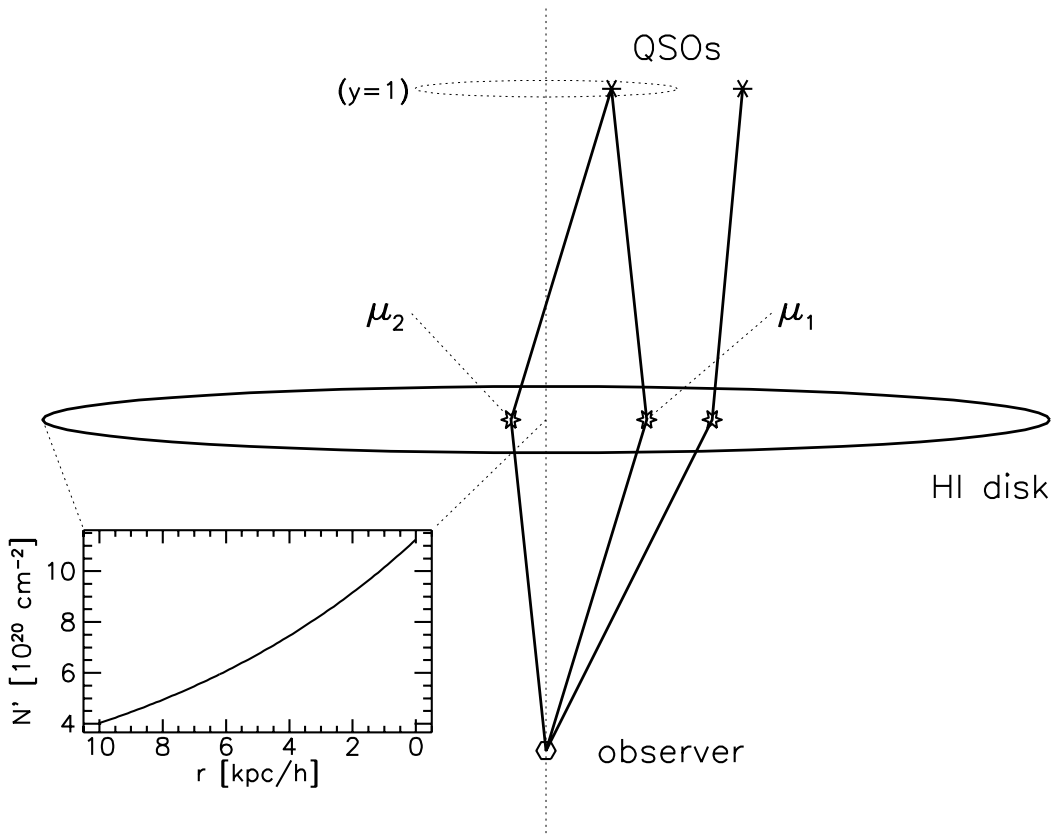


Figure 1.— Schematic illustration of the lensing geometry. QSOs in the source plane are either multiply or singly imaged, depending on their distance from the optical axis. The two corresponding regions in the source plane are separated by the dotted curve, marked  $y = 1$ . Light rays are magnified by the lens on their way to the observer. The magnification factors,  $\mu_1$  and  $\mu_2$ , of the two images of the central QSO are indicated for further reference. The inserted figure displays the face-on hydrogen column density as a function of radius in the HI disk.

We further assume that each light ray which passes an intervening absorption system face-on within a radius  $R_{\text{H}}(N')$  from its center shows damped Ly $\alpha$  absorption with a column density equal to or greater than  $N'$ . Following common practice (e.g., Lanzetta et al. 1991; Wolfe et al. 1986), we take  $R_{\text{H}}(N')$  to be proportional to the optical radius  $R_*$ , and the optical radius to be proportional to some power  $t$  of the luminosity of the system,

$$R_{\text{H}}(N') = f_{\text{H}}(N') R_* \ell^t, \quad (2.3)$$

where  $R_*$  is the optical radius of an  $L_*$  galaxy. Observations suggest the values (e.g., Holmberg 1975; Peterson, Strom, & Strom 1979; Broeils & van Woerden 1994)

$$R_* \approx 11 h^{-1} \text{ kpc} \quad , \quad t \approx 0.4. \quad (2.4)$$

Measurements of the surface density of neutral hydrogen in local disk galaxies (e.g., Broeils & van Woerden 1994) suggest that the surface density of neutral hydrogen is well fitted by an exponential function of radius. Figure 8b of Broeils & van Woerden (1994) shows average HI profiles such that

$$f_{\text{H}}(N') = \frac{3}{2} - 2 \log \left( \frac{N'}{2 \times 10^{20} \text{ cm}^{-2}} \right) \quad (2.5)$$

describes reasonably well the average disk radius within which the neutral-hydrogen column density exceeds  $N'$ . Note that  $N'$  is the face-on column density of the neutral-hydrogen disk. If the disk is inclined by an angle  $\theta$  relative to the line-of-sight, the observed column density is  $N = N' / \cos \theta$ . We neglect the finite scale-height of the hydrogen disk, which is typically smaller by 1–2 orders of magnitude than the disk radius. The geometrical cross section  $\sigma_{\text{Ly}\alpha}(N)$  of a disk inside of which the observed column density exceeds  $N$  is obtained by averaging over all inclination angles,

$$\sigma_{\text{Ly}\alpha}(N) = \pi R^2 \int_0^1 d\gamma f_{\text{H}}^2(N\gamma) \gamma \text{H}(\gamma - \gamma_0), \quad (2.6)$$

where  $\gamma \equiv \cos \theta$ , and the Heaviside step function  $\text{H}(\gamma - \gamma_0)$  accounts for the fact that very high column densities can only be observed in disks which are inclined by an angle  $\theta \geq \theta_0$ , with

$$\gamma_0 \equiv \cos \theta_0 = \min \left[ 1, 10^{3/4} \left( \frac{2 \times 10^{20} \text{ cm}^{-2}}{N} \right) \right]. \quad (2.7)$$

Evaluating the average in equation (2.6), we obtain

$$\sigma_{\text{Ly}\alpha}(N) = \pi R^2 \langle f_{\text{H}}^2(N) \rangle, \quad (2.8)$$

where

$$\langle f_{\text{H}}^2(N) \rangle^{1/2} = \frac{\gamma_0}{2} \left[ f_{\text{H}}^2(N) - 2f_{\text{H}}(N) \frac{2 \ln \gamma_0 - 1}{\ln 10} + \frac{2}{\ln^2 10} (1 - 2 \ln \gamma_0 + 2 \ln^2 \gamma_0) \right]^{1/2}. \quad (2.9)$$

We define the angle-averaged disk radius for absorption with column density  $\geq N$  by

$$\langle R_{\text{H}}(N) \rangle = R \langle f_{\text{H}}^2(N) \rangle^{1/2}. \quad (2.10)$$

We model the lensing properties of the intervening systems as singular isothermal spheres, assuming that these systems resemble galactic disks with flat rotation curves which are embedded in spherical halos. Such systems are the simplest to consider, as they are characterized by only one parameter, viz. their one-dimensional velocity dispersion,  $\sigma_v$ . *HST* observations of bulges of spiral galaxies show no indication for cores, i.e., central regions in which the surface-brightness is constant (Tremaine et al. 1995, in preparation). Similarly, models for observed gravitational-lens systems indicate that the density profiles of the lenses are either singular or have very small core radii  $\lesssim 200$  pc (Rix, Schneider, & Bahcall 1992; Kochanek 1991). Assuming a circular rotational velocity of  $v_{c,*} = 220$  km s $^{-1}$  for an  $L_*$  galaxy (e.g., Peebles 1993; Aaronson, Huchra, & Mould 1979), we get

$$\sigma_{v,*} = \frac{v_{c,*}}{\sqrt{2}} \approx 160 \text{ km s}^{-1} . \quad (2.11)$$

The rotational velocity, and hence the velocity dispersion, are related to the luminosity through the Tully-Fisher relation (Tully & Fisher 1977),

$$\sigma_v = \ell^{1/\alpha} \sigma_{v,*} . \quad (2.12)$$

The Tully-Fisher exponent  $\alpha$  depends on the waveband where the observations are taken; it ranges from  $\alpha \approx 2$  in the blue to  $\alpha \approx 4$  in the infrared (see Strauss & Willick 1995, and references therein).

## 2.2. Probability for Damped Ly $\alpha$ Absorption

Ignoring gravitational lensing, the probability for a QSO to exhibit damped Ly $\alpha$  absorption in its spectrum can be calculated by dividing the physical path length surveyed for absorption by the mean free path between subsequent absorptions,

$$P_{\text{Ly}\alpha}(N) = n_{\text{Ly}\alpha} \sigma_{\text{Ly}\alpha}(N) \Delta X , \quad (2.13)$$

where  $n_{\text{Ly}\alpha}$  is the spatial density of absorbers and  $\sigma_{\text{Ly}\alpha}(N)$  is their individual cross section for damped Ly $\alpha$  absorption with a column density  $\geq N$ , given by equation (2.8). Integrating over galaxy luminosities we find

$$n_{\text{Ly}\alpha} \sigma_{\text{Ly}\alpha}(N) = \Phi_* \Gamma(1 + s + 2t) \pi R_*^2 \langle f_{\text{H}}^2(N) \rangle , \quad (2.14)$$

where the Gamma function results from the Schechter luminosity function, taking the luminosity dependence of  $R$  into account. The physical path length between redshifts  $z_1$  and  $z_2$  is given by the absorption-distance difference,

$$\Delta X(z_1, z_2) = \int_{z_1}^{z_2} dz (1+z)^3 \left| \frac{c dt}{dz} \right| , \quad (2.15)$$

where the factor  $(1+z)^3$  accounts for the change in the galaxy density due to the cosmological expansion. The proper-distance interval  $|c dt|$  depends on the cosmological parameters,

$$|c dt| = \frac{c}{H_0} \frac{dz}{1+z} \frac{1}{\sqrt{\Omega_0(1+z)^3 + (1 - \Omega_0 - \Omega_\Lambda)(1+z)^2 + \Omega_\Lambda}} , \quad (2.16)$$

where  $\Omega_0$  is the present-day density parameter, and  $\Omega_\Lambda$  is the cosmological constant. Combining the last four equations, we obtain

$$P_{\text{Ly}\alpha}(z_1, z_2, N) = \Phi_* \Gamma(1 + s + 2t) \pi R_*^2 \langle f_{\text{H}}^2(N) \rangle \int_{z_1}^{z_2} dz (1+z)^3 \left| \frac{c dt}{dz} \right| ; \quad (2.17)$$

(see also Bahcall & Peebles 1969, and Burbidge et al. 1977). Note that  $P_{\text{Ly}\alpha}(z_1, z_2, N)$  is independent of the Hubble constant.

This equation changes considerably when gravitational lensing is taken into account due to the magnification bias. The derivation of the absorption probability can then be split into two steps; one to calculate the probability for magnification, and the second to convolve the magnification probability with the QSO number counts.

We adopt the conventional description of gravitational lensing (e.g., Schneider et al. 1992). The optical axis of the lens system is defined by the positions of the observer and the center of the lens, and the lens- and source planes are constructed orthogonal to the optical axis at the redshifts  $z$  and  $z_s$  of the lens and the source, respectively. Later, we shall refer to  $z$  and  $z_s$  by the redshifts of the absorbers,  $z_{\text{abs}}$ , and the QSOs,  $z_{\text{QSO}}$ . The lens plane constitutes the observer's sky in the vicinity of the lens. We normalize the coordinates in the lens plane by the length scale appropriate for singular isothermal spheres,

$$\xi_0 \equiv 4\pi \left( \frac{\sigma_v}{c} \right)^2 \frac{c}{H_0} \frac{r_d r_{ds}}{r_s} \equiv 4\pi \left( \frac{\sigma_v}{c} \right)^2 \frac{c}{H_0} d(z, z_s) , \quad (2.18)$$

where  $r_d, r_s$ , and  $r_{ds}$  are the angular-diameter distances from the observer to the lens (deflector) and the source planes, and from the lens to the source plane, respectively, in units of the Hubble length ( $c/H_0$ ). For a detailed description of the lensing properties of singular isothermal spheres, see §8.1 of Schneider et al. (1992). Coordinates in the source plane are correspondingly scaled by the projection of  $\xi_0$  from the lens- onto the source plane. Using equation (2.12), the length scale  $\xi_0$  can be written as

$$\xi_0 = 4\pi \left( \frac{\sigma_{v,*}}{c} \right)^2 \frac{c}{H_0} d(z, z_s) \ell^{2/\alpha} \equiv \frac{c}{H_0} \theta_* d(z, z_s) \ell^{2/\alpha} . \quad (2.19)$$

We denote the scaled coordinates in the lens and source planes by  $x$  and  $y$ , respectively. Then, sources with  $y \leq 1$  have two images at  $x = y \pm 1$ , while sources outside  $y = 1$  have a single image at  $x = y + 1$ . The total magnification of a point source is

$$\mu = \begin{cases} 2/y & (y \leq 1) \\ 1 + 1/y & (\text{otherwise}) \end{cases} . \quad (2.20)$$

If a source is multiply imaged, and if the multiple images are not resolved when the spectrum of the source is taken, then the damped Ly $\alpha$  absorption of the two superposed spectra is dominated by that of the brighter image which is formed at the larger impact parameter,  $x = y + 1$ . In order to get damped Ly $\alpha$  absorption with column density  $\geq N$  in the composite spectrum, the outer image of the source must lie at a sufficiently small impact parameter. This is equivalent to the requirement

$$y \leq y_{\text{H}}(N) = x_{\text{H}}(N) - 1 = \frac{\langle R_{\text{H}}(N) \rangle}{\xi_0} - 1 . \quad (2.21)$$

Inserting equations (2.3), (2.10), and (2.19) into (2.21), we obtain

$$y_{\text{H}}(z, z_{\text{s}}, N) = \frac{H_0 R_* \langle f_{\text{H}}^2(N) \rangle^{1/2}}{c \theta_* d(z, z_{\text{s}})} \ell^{t-2/\alpha} - 1. \quad (2.22)$$

For reasonable choices of  $t$  and  $\alpha$ ,  $(t - 2/\alpha) \approx 0$ , so that  $y_{\text{H}}(z, z_{\text{s}}, N)$  depends only weakly on  $\ell$ . In the following, we shall assume that  $y_{\text{H}}(z, z_{\text{s}}, N)$  is independent of  $\ell$  since this simplifies our discussion considerably.

The dimensionless cross section of the intervening system for magnifying a point source by more than a factor  $\mu$  and causing damped Ly $\alpha$  absorption with a column density of  $\geq N$  is defined to be the corresponding area in the source plane within which a point source has to lie, normalized by the square of the length scale in the source plane. For the singular isothermal sphere, the cross section is given by (cf. Schneider et al. 1992)

$$\sigma(z, z_{\text{s}}, N; \mu) = \begin{cases} 4\pi/\mu^2 & [\mu \geq 2/y_{\text{H}}(z, z_{\text{s}}, N)] \\ \pi y_{\text{H}}^2(z, z_{\text{s}}, N) & (\text{otherwise}) \end{cases}, \quad (2.23)$$

if  $y_{\text{H}}(z, z_{\text{s}}, N) \leq 1$ , or by

$$\sigma(z, z_{\text{s}}, N; \mu) = \begin{cases} 4\pi/\mu^2 & (\mu \geq 2) \\ \pi/(\mu - 1)^2 & [2 > \mu \geq 1 + 1/y_{\text{H}}(z, z_{\text{s}}, N)] \\ \pi y_{\text{H}}^2(z, z_{\text{s}}, N) & (\text{otherwise}) \end{cases} \quad (2.24)$$

if  $y_{\text{H}}(z, z_{\text{s}}, N) > 1$ .

The probability for a QSO to be magnified by more than  $\mu$  and at the same time to show damped Ly $\alpha$  absorption with column density  $\geq N$  in its spectrum can now be found by calculating the fraction of the total area of the source sphere covered by the appropriate cross sections of the lens population. Implicitly, this assumes that lenses and QSOs are physically uncorrelated and that the cross sections do not significantly overlap; both of these assumptions are well justified. Integrating over source luminosity and redshift between redshifts  $z_1$  and  $z_2 \leq z_{\text{s}}$ , we obtain the probability that a QSO at redshift  $z_{\text{s}}$  shows damped Ly $\alpha$  absorption with column density  $\geq N$ , and is magnified by a factor  $\geq \mu$  by lenses in the redshift interval  $z_1 \leq z \leq z_2$ ,

$$P'_{\text{GL}}(z_1, z_2, z_{\text{s}}, N; \mu) = \left(\frac{c}{H_0}\right)^2 \Phi_* \theta_*^2 \Gamma\left(1 + s + \frac{4}{\alpha}\right) \times \int_{z_1}^{z_2} dz d^2(z, z_{\text{s}}) (1+z)^3 \left| \frac{c dt}{dz} \right| \sigma(z, z_{\text{s}}, N; \mu) \quad (2.25)$$

As in equation (2.14), the Gamma function results from integrating over luminosity, assuming that the dimensionless magnification cross section is independent of  $\ell$ .

Equation (2.17) should be a limiting case of equation (2.25) in the sense that if we disregard lensing, (2.25) should equal (2.17). In fact, if we allow for any magnification factor by setting  $\mu \rightarrow 1$ , the cross section is limited by the column-density requirement only, and we obtain from equations (2.23) or (2.24)

$$\sigma(z, z_{\text{s}}, N; \mu) \rightarrow \pi y_{\text{H}}^2(z, z_{\text{s}}, N). \quad (2.26)$$

If  $\mu \rightarrow 1$ , we further have  $y_{\text{H}}(z, z_{\text{s}}, N) \gg 1$ , and thus

$$\sigma(z, z_{\text{s}}, N; \mu) \rightarrow \pi \langle f_{\text{H}}^2(N) \rangle R_*^2 \left[ \frac{H_0}{c \theta_* d(z, z_{\text{s}})} \right]^2. \quad (2.27)$$

Inserting this into equation (2.25), we obtain

$$P'_{\text{GL}}(z_1, z_2, z_{\text{s}}, N; \mu) \rightarrow \Phi_* \Gamma \left( 1 + s + \frac{4}{\alpha} \right) \pi R_*^2 \langle f_{\text{H}}^2(N) \rangle \int_{z_1}^{z_2} dz (1+z)^3 \left| \frac{c dt}{dz} \right|, \quad (2.28)$$

which is identical with equation (2.17) provided that  $t \approx 2/\alpha$ , as we have assumed before for simplicity. Note, however, that lensing reduces the area in the source plane within which QSOs show damped Ly $\alpha$  absorption with column density  $\geq N$  because of the focusing effect of the lens. More precisely, this area is reduced compared to the case when lensing is ignored by the average magnification factor within  $y_{\text{H}}(z, z_{\text{s}}, N)$ .

Let now  $(dN_{\text{QSO}}/dS)(S) dS$  be the intrinsic number of QSOs at redshift  $z_{\text{s}}$  with flux between  $S$  and  $S + dS$ . Due to the magnification bias, the observed number of QSOs with flux greater than  $S$  which show damped Ly $\alpha$  absorption with column density  $\geq N$  between redshifts  $z_1$  and  $z_2$  is given by

$$N'_{\text{QSO}}(S) = \int_0^\infty dS' P'_{\text{GL}} \left( z_1, z_2, z_{\text{s}}, N; \frac{S}{S'} \right) \frac{dN_{\text{QSO}}}{dS}(S') \quad (2.29)$$

(see, e.g. Schneider et al. 1992; Narayan & Wallington 1993). Therefore, the probability for a QSO at redshift  $z_{\text{s}}$  to be detected with a flux greater than  $S$  and to show damped Ly $\alpha$  absorption with column density greater than  $N$  is given by

$$P_{\text{GL}}(z_1, z_2, z_{\text{s}}, N; S) = \frac{1}{N_{\text{QSO}}(S)} \int_0^\infty dS' P'_{\text{GL}} \left( z_1, z_2, z_{\text{s}}, N; \frac{S}{S'} \right) \frac{dN_{\text{QSO}}}{dS}(S'). \quad (2.30)$$

If we disregard gravitational lensing,  $P_{\text{GL}}(z_1, z_2, z_{\text{s}}, N; S)$  reduces to equation (2.17) and becomes independent of the QSO flux  $S$ .

The intrinsic QSO number counts are well modeled by a broken power law (e.g., Boyle, Shanks, & Peterson 1988, Hartwick & Schade 1990)

$$\frac{dN_{\text{QSO}}}{dS}(S) = \begin{cases} S^{-a} & (S \leq S_0) \\ S^{-b} & (\text{otherwise}) \end{cases}, \quad (2.31)$$

where  $a = 1.64$  and  $b = 3.52$  provide a reasonable fit to observational data (Pei 1995). The break luminosity  $S_0$  corresponds to an apparent QSO magnitude of  $B \approx 19.5$ .

### 2.3. Inferred Properties of Damped Ly $\alpha$ Absorbers

One of the goals of observing Ly $\alpha$  absorbers is to infer the amount of neutral hydrogen in the universe, and thereby to study the history of systems which contain neutral hydrogen. An intermediate step in this calculation is to derive the column-density distribution function  $f(N)$  of the absorbers, which is defined to be the number of absorbers with column density within  $dN$  of  $N$  per unit absorption distance  $dX$ . Using the definition of the absorption distance, the probability without lensing (2.17) can be written as

$$P_{\text{Ly}\alpha}(z_1, z_2, N) = \Phi_* \Gamma(1 + s + 2t) \pi R_*^2 \langle f_{\text{H}}^2(N) \rangle [X(z_2) - X(z_1)] . \quad (2.32)$$

If among a sample of  $q$  QSOs  $l$  damped Ly $\alpha$  absorbers are found within a column-density range of  $\Delta N$  around  $N$ , and if the absorption distance surveyed per QSO is  $\Delta X(z_1, z_2)$ , then the column-density distribution inferred from these observations is given by

$$f(N) dN dX = \frac{c}{H_0} \frac{l}{q \Delta X(z_1, z_2) \Delta N} dN dX . \quad (2.33)$$

Since  $(l/q)$  approximates the probability for a QSO to show the specified absorption, we can write

$$f(N) = \frac{c}{H_0} \frac{1}{\Delta X(z_1, z_2)} \left| \frac{\partial P(z_1, z_2, N)}{\partial N} \right| . \quad (2.34)$$

Note that  $f(N)$  scales linearly with the value of the Hubble constant, because  $P$  is independent of  $H_0$  and  $\Delta X$  is proportional to  $H_0^{-1}$ . Ignoring gravitational lensing, equation (2.32) can be substituted into equation (2.34) to give

$$f_{\text{Ly}\alpha}(N) = \frac{c}{H_0} \Phi_* \Gamma(1 + s + 2t) \pi R_*^2 \left| \frac{\partial \langle f_{\text{H}}^2(N) \rangle}{\partial N} \right| . \quad (2.35)$$

This result is independent of the QSO redshift, the QSO flux, and the redshift interval surveyed for damped Ly $\alpha$  absorption. If, however, gravitational lensing is taken into account, equation (2.34) reads

$$f_{\text{GL}}(z_1, z_2, z_s, S; N) = \frac{c}{H_0} \frac{1}{\Delta X(z_1, z_2)} \left| \frac{\partial P_{\text{GL}}(z_1, z_2, z_s, N; S)}{\partial N} \right| . \quad (2.36)$$

The resulting column-density distribution depends on the redshifts selected, the cosmological parameters, and, in particular, on the QSO flux  $S$  because of the magnification bias.

Given  $f(N)$ , the inferred comoving density of neutral hydrogen in systems with column densities of  $N_1 \leq N \leq N_2$ , normalized by the present critical density, is found to be

$$\Omega_{\text{HI}}(N_1, N_2) = \frac{H_0}{c} \frac{\bar{m}}{\rho_{c,0}} \int_{N_1}^{N_2} dN N f(N) , \quad (2.37)$$

where  $\bar{m}$  is the mean molecular mass per proton, and  $\rho_{c,0}$  is the present-day closure density,

$$\rho_{c,0} = \frac{3H_0^2}{8\pi G} . \quad (2.38)$$

The lower integration bound is fixed by the requirement that the absorption be damped, i.e.  $N_1 \sim 10^{20} \text{ cm}^{-2}$ . In principle, the choice of  $N_2$  is arbitrary, but in existing surveys it is limited to  $N_2 \lesssim 10^{22} \text{ cm}^{-2}$ . Since  $f(N)$  scales linearly with the Hubble constant,  $\Omega_{\text{HI}}$  is independent of  $H_0$ .

The fact that  $f(N)$  depends on the redshifts chosen and the QSO flux when gravitational lensing is taken into account implies that the inferred value of  $\Omega_{\text{HI}}$  depends on these parameters.

### 3. Results

Based on the formalism developed in §2, we now consider quantitatively the characteristic signatures imprinted by gravitational lensing upon quantities inferred from studies of damped Ly $\alpha$  absorption systems. We begin with the column-density distribution function,  $f(N)$ . Figure 2 shows  $N f(N)$  for two choices for the absorber-redshift interval and for three cosmological models. We fix the QSO redshift at  $z_{\text{QSO}} = 3$  and consider the absorber-redshift intervals of  $2 \leq z_{\text{abs}} \leq 3$  (Fig. 2a) and  $0.4 \leq z_{\text{abs}} \leq 1$  (Fig. 2b). The heavy line in both panels of figure 2 shows  $N f(N)$  ignoring gravitational lensing, and the three additional curves display the effect of lensing for the cosmological models  $\Omega_0 = 1$ ,  $\Omega_A = 0$  (solid line);  $\Omega_0 = 0.2$ ,  $\Omega_A = 0$ , (dotted line); and  $\Omega_0 = 0.2$ ,  $\Omega_A = 0.8$  (dashed line).

The observed column-density distribution of Ly $\alpha$  absorbers can be well fitted by a power law over a broad range of column densities,  $f(N) \propto N^\beta$  with  $\beta = -1.7 \pm 0.2$  (Tytler 1987; Lanzetta et al. 1991). Our results for  $f(N)$  reproduce this power-law behavior well for  $N \lesssim 10^{21} \text{ cm}^{-2}$  where the effect of lensing is weak. This indicates that our modeling of the neutral-hydrogen profiles in galactic disks is reasonable.

For high-redshift absorbers ( $z_{\text{abs}} \lesssim z_{\text{QSO}}$ ),  $N f(N)$  drops below the result expected without lensing at  $N \sim 10^{21} \text{ cm}^{-2}$ , then rises to a peak around  $N \sim 10^{22} \text{ cm}^{-2}$ , and finally declines sharply at still larger  $N$ . As mentioned in §2, the area in the source plane within which QSOs show damped Ly $\alpha$  absorption with a given column density is reduced compared to the geometric cross section by the focusing effect of gravitational lensing. The magnification bias compensates this reduction for increasing  $N$ , because lines-of-sight passing through higher column densities experience higher magnifications on average. The magnification bias is weak for high-redshift absorbers (cf. Fig. 2a). However, for low-redshift absorbers and high-redshift QSOs, lensing by the absorbers is much more efficient, so that the peak in  $N f(N)$ , produced by the magnification bias, is much more pronounced (cf. Fig. 2b). For column densities beyond the peak location,  $N f(N)$  sharply cuts off. If the QSO is singly imaged, the ray-bending due to the lens increases the impact parameter of the QSO image compared to the case of inefficient lensing. If the QSO is multiply imaged, the brighter image whose spectrum dominates the absorption feature is also formed at a larger distance from the center of the lens than in the unlensed case. Thus, the lens prevents the light of the dominant image from passing through the highest column-density regions of the galactic disks, so that the highest column densities cannot be traversed by the dominant fraction of the QSO light.

Since  $y_{\text{H}} \geq 0$ , equation (2.21) requires that

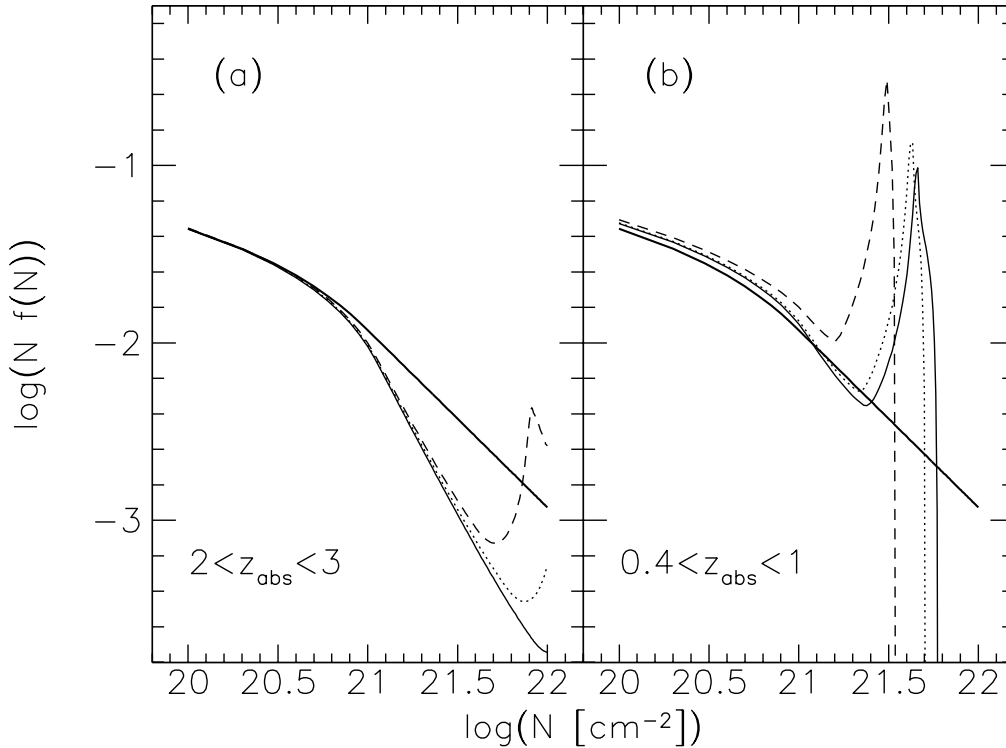


Figure 2.— Column-density distribution of damped Ly $\alpha$  absorbers per logarithmic column-density interval,  $N f(N)$ , for  $H_0 = 50 \text{ km s}^{-1} \text{ Mpc}^{-1}$ . The integral of this function is proportional to the cosmological density of neutral hydrogen,  $\Omega_{\text{HI}}$ . The heavy curve in both panels displays  $N f(N)$  without the influence of gravitational lensing. The three other curves were calculated for three different cosmological models, taking gravitational lensing into account. The cosmological model parameters are:  $\Omega_0 = 1$ ,  $\Omega_A = 0$  (solid line);  $\Omega_0 = 0.2$ ,  $\Omega_A = 0$  (dotted line); and  $\Omega_0 = 0.2$ ,  $\Omega_A = 0.8$  (dashed line). In both panels, the QSO redshift is fixed at  $z_{\text{QSO}} = 3$ . In panel (a), the redshift interval for the absorbers is  $2 \leq z_{\text{abs}} \leq 3$ , and in panel (b),  $0.4 \leq z_{\text{abs}} \leq 1$ . While the influence of lensing is weak for high-redshift absorbers, a pronounced peak followed by a sharp cut-off arises for low-redshift absorbers. The QSO magnitude threshold is  $B = 16$ . We ignore the effect of possible obscuration by dust.

$$\xi_0 \leq \langle R_{\text{H}}(N) \rangle \quad (3.1)$$

for such lenses which contribute to damped Ly $\alpha$  absorption with a column density  $\geq N$ . This implies that the maximum lensing efficiency of the absorbers is achieved for a column density  $N_{\text{peak}}$  such that

$$\max_{z_1 \leq z \leq z_2} \xi_0 = \langle R_{\text{H}}(N_{\text{peak}}) \rangle. \quad (3.2)$$

For  $N > N_{\text{peak}}$ , the redshift range for possible absorbers is clipped, so that their number decreases. The highest accessible column density  $N_{\text{cut}}$  is reached once

$$\min_{z_1 \leq z \leq z_2} \xi_0 = \langle R_{\text{H}}(N_{\text{cut}}) \rangle. \quad (3.3)$$

If  $\min \xi_0 = 0$ , arbitrarily high column densities can appear, but only in an arbitrarily small number of absorbers. Therefore, the peak of  $f(N)$  at  $N_{\text{peak}}$  is then followed by a decrease

with a finite slope for higher  $N$ . If  $\min \xi_0$  is finite, there exists a finite upper limit  $N_{\text{cut}}$  to the accessible column densities, where  $f(N)$  is steeply cut off. The minimum value of  $\xi_0$  can vanish if and only if  $z_1 = 0$  or  $z_2 = z_{\text{QSO}}$ , as is the case in figure 2a. In all other cases,  $f(N)$  is cut off at a finite column density  $N_{\text{cut}}$ , as shown in figure 2b. Moreover, since  $\xi_0 \propto \sigma_v^2$ , the peak location measures the velocity dispersion and thus the depth of the gravitational potential of the absorber.

In reality, the sharp peaks apparent in figure 2 may be broadened due to possible clumpiness of the HI distribution or due to an average over different density profiles of disk galaxies of different morphological types (see Broeils & van Woerden 1994). This smoothing of the peaks may render it difficult to constrain the value of the cosmological constant just from the measured location of the peaks. It is also important to note that for column densities  $\gtrsim 10^{22} \text{ cm}^{-2}$ , the potential obscuration of the QSOs by dust is expected to be strong and therefore should be taken into account (Fall, Pei, & McMahon 1989; Pei, Fall, & Bechtold 1991; Fall & Pei 1993). The dust obscuration tends to reduce the observed number of QSOs with high column-density absorbers. Although this effect has the opposite sign to that of the magnification bias, its impact on the predicted  $f(N)$  is limited because of the sharp cut-off introduced by the bending of light rays due to lensing. We discuss this issue further in §4. We do not include a model for the dust obscuration in figure 2 because the central opacity of nearby disk galaxies is still a subject of current debate (e.g. Byun 1993; Davies et al. 1993; Byun, Freeman, & Kylafis 1994; Jansen et al. 1994; Rix 1994), and the evolution of this opacity with redshift is even more uncertain.

The distortion of the column-density distribution due to lensing affects the inferred value of the cosmological density parameter in neutral hydrogen,  $\Omega_{\text{HI}}$ . Figure 3 shows the ratio between the inferred and the true value of  $\Omega_{\text{HI}}$  for two choices for the absorber-redshift interval and for the three cosmological models specified before. Similar to observational studies (e.g., Lanzetta et al. 1995), we calculate the contribution to  $\Omega_{\text{HI}}$  of damped absorption systems with  $20 \leq \log(N \text{ cm}^2) \leq 22$ . In figure 3a, we consider the absorber redshift interval  $0 \leq z_{\text{abs}} \leq 1$  while the QSO redshift ranges between  $1 \leq z_{\text{QSO}} \leq 3$ . In figure 3b, the QSO redshift varies in the range  $0 \leq z_{\text{QSO}} \leq 3$ , and the absorber redshifts range within  $0 \leq z_{\text{abs}} \leq z_{\text{QSO}}$ .

The most prominent feature in both panels is the artificial decline of the inferred value of  $\Omega_{\text{HI}}$  with decreasing redshift, imitating a strong evolution of the neutral-hydrogen density with redshift. This noticeable effect arises because  $\Omega_{\text{HI}}$  is dominated by the high column-density absorbers, for which gravitational lensing can strongly influence the result due to the magnification bias. While  $\Omega_{\text{HI}}$  is generally overestimated for  $z_{\text{QSO}} \gtrsim 0.5$ , it can also be significantly underestimated for lower QSO redshifts. The reason for this underestimate is that the peak in  $f(N)$  shifts towards higher  $N$  for smaller QSO redshifts. This follows because the lensing length scale  $\xi_0$  becomes smaller, requiring  $R_{\text{H}}(N)$  to be smaller and therefore  $N$  to be larger for high magnifications to arise. If the peak column density becomes larger than  $N_2$ , the inferred  $\Omega_{\text{HI}}$  rapidly drops below its true value (see Fig. 2).

The discrepancies between the inferred and the true values of  $\Omega_{\text{HI}}$  are strongest in case of a non-zero cosmological constant, as shown by the dashed curves. It is interesting that the artificial evolution in the apparent  $\Omega_{\text{HI}}(z)$  is already comparable to that observed

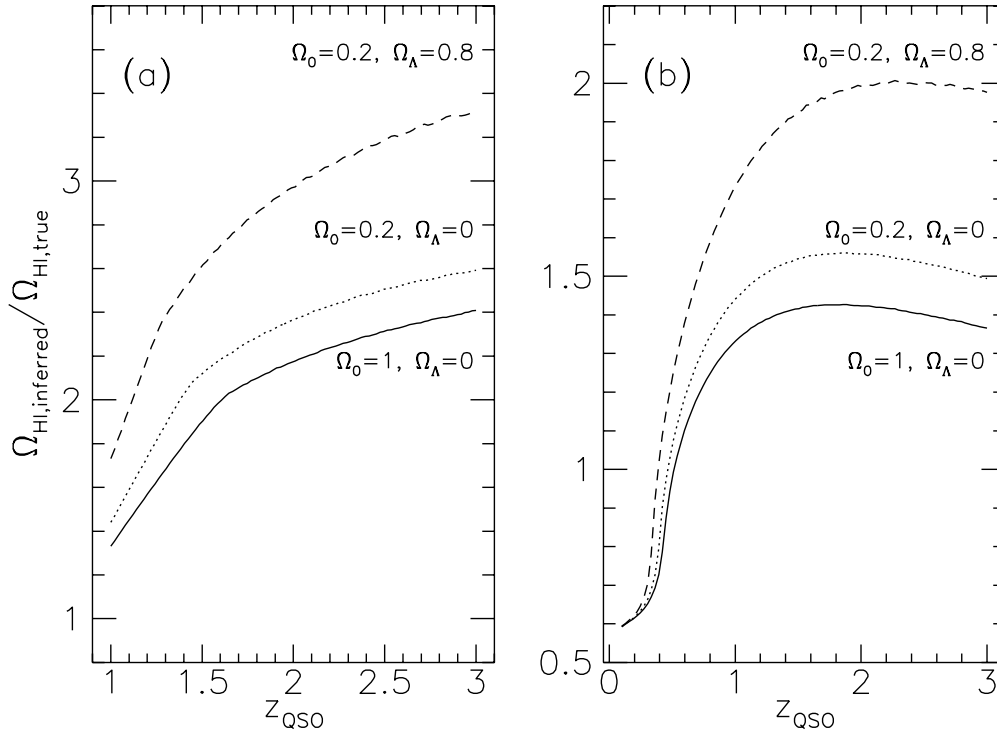


Figure 3.— The ratio between the inferred and the true cosmological density parameter in neutral hydrogen,  $\Omega_{\text{HI}}$ , is shown for two different choices of the absorber redshifts and the three cosmological models considered in figure 2. In the panel (a), we average the result over absorber redshifts in the interval  $0 \leq z_{\text{abs}} \leq 1$ , while the QSO redshift is increased from  $z_{\text{QSO}} = 1$  to  $z_{\text{QSO}} = 3$ . In panel (b), the QSO redshifts range within  $0 \leq z_{\text{QSO}} \leq 3$ , while the absorber redshifts lie between zero and  $z_{\text{QSO}}$ . In both cases, the inferred density parameter decreases at low redshifts. For low QSO redshifts,  $z_{\text{QSO}} < 0.5$ , the inferred density parameter underestimates the true HI density, but for  $z_{\text{QSO}} > 0.5$ , the neutral-hydrogen density is overestimated. A limiting QSO magnitude of  $B = 16$  was assumed. For the sensitivity of the result to the QSO magnitude threshold, see figure 5.

(White et al. 1993; Bahcall et al. 1993; Lanzetta et al. 1995), even before including any plausible amount of gas consumption by star formation (e.g., Kauffmann & Charlot 1994; Lanzetta et al. 1995). Although the observed evolution is often expressed in terms of  $\Omega_{\text{HI}}$  as a function of  $z_{\text{abs}}$  rather than  $z_{\text{QSO}}$ , the previous searches were constrained to find high-redshift absorbers in the spectra of high-redshift QSOs (using ground-based observations), and bright low-redshift QSOs in surveys of low-redshift absorbers (using *IUE* data).

The expected redshift distribution of the damped Ly $\alpha$  absorption systems is presented in figure 4, given two choices of the absorber-redshift intervals. For the curves in figure 4a,  $2 \leq z_{\text{abs}} \leq 3$ , and for the curves in figure 4b,  $0 \leq z_{\text{abs}} \leq 1$ . In both cases, the QSO redshift is kept fixed at  $z_{\text{QSO}} = 3$ . The solid curves show the result derived including lensing, while lensing was ignored for the dashed curves. Only results for the cosmological model with  $\Omega_0 = 0.2$  and  $\Omega_{\Lambda} = 0$  are shown because for this model the difference between the lensed and unlensed cases is intermediate (cf. Fig. 3). Both panels suggest that it

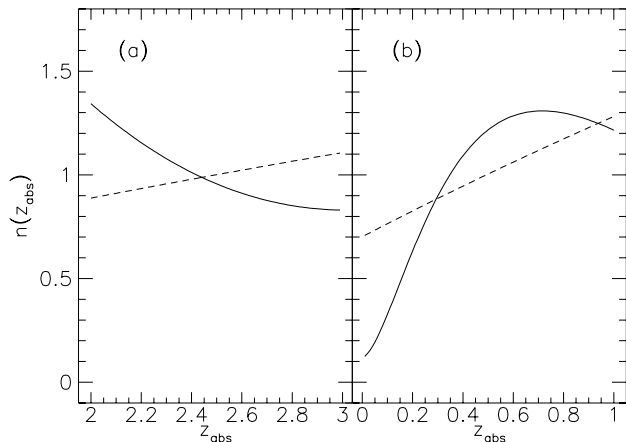


Figure 4.— Normalized redshift distribution of damped Ly $\alpha$  absorbers in the spectra of QSOs at a redshift  $z_{\text{QSO}} = 3$ , for absorbers at either high redshifts,  $2 \leq z_{\text{abs}} \leq 3$  (panel a) or low-redshifts,  $0 \leq z_{\text{abs}} \leq 1$  (panel b). In both panels, the dashed curve was derived ignoring gravitational lensing, while the solid curves were derived including lensing. Only results for the cosmological parameters  $\Omega_0 = 0.2$ ,  $\Omega_A = 0$  are shown. The curves are arbitrarily normalized to unit area.

might be difficult to distinguish between the lensed and unlensed cases on the basis of the absorber-redshift distribution alone. Especially if  $\Omega_A$  is small, the curves are virtually indistinguishable given any reasonable error bars in the actual data. In addition, allowing for a range of QSO redshifts would tend to smear out and further reduce the difference between the two curves.

The insensitivity of the absorber-redshift distribution to lensing (cf. Fig. 4), and the weakness of the distortion of  $f(N)$  due to lensing for high-redshift absorbers (cf. Fig. 2a), offer a plausible explanation as to why these imprints of lensing were not identified observationally in the past. The lensing signatures would be most significant in samples of bright, high-redshift QSOs which are surveyed for low-redshift, damped Ly $\alpha$  absorption with  $z_{\text{abs}} \lesssim 1$ . Unfortunately, existing surveys of damped Ly $\alpha$  systems (e.g., Lanzetta et al. 1995) do not include a sufficiently large number of cases with  $z_{\text{QSO}} \gtrsim 2-3$  and  $z_{\text{abs}} \lesssim 1$ . However, it should be straightforward to design a search strategy for the purpose of detecting the lensing signature, because high column-density absorbers and bright QSOs are both easy to detect.

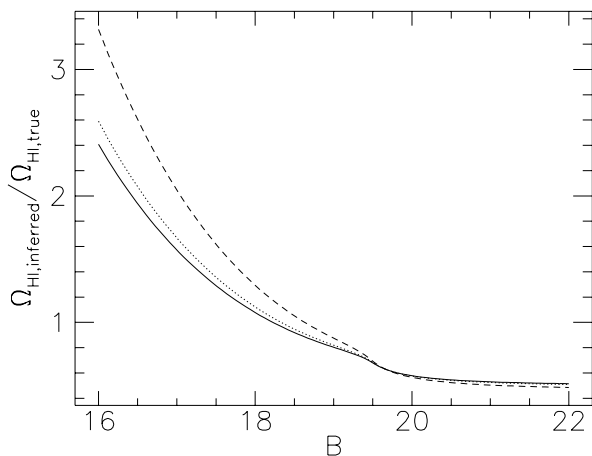


Figure 5.— The inferred neutral-hydrogen density parameter depends on the limiting magnitude  $B$  of the QSO sample due to lensing. We consider a QSO redshift  $z_{\text{QSO}} = 3$  and absorbers in the redshift interval  $0 \leq z_{\text{abs}} \leq 1$ . The three curves show the ratio between the inferred and the true  $\Omega_{\text{HI}}$  for the three cosmological models used in figure 2.

Since the amplitude of the magnification bias depends on the QSO brightness, the

inferred value of  $\Omega_{\text{HI}}$  depends on the magnitude limit of the QSO sample. The three curves in figure 5 show this dependence for the three cosmological models considered before. We assume  $z_{\text{QSO}} = 3$  and  $0 \leq z_{\text{abs}} \leq 1$ . The figure shows that the value of  $\Omega_{\text{HI}}$  can be substantially overestimated for a bright QSO sample, but can also be underestimated if the QSO sample is faint. The latter effect occurs because the area in the source plane within which QSOs show damped Ly $\alpha$  absorption with column density  $\geq N$  is reduced due to the focusing effect of the lens, as described before. The dependence of  $\Omega_{\text{HI}}$  on the magnitude limit of the QSO sample can be used to separate evolutionary effects in the absorber population from effects caused by gravitational lensing.

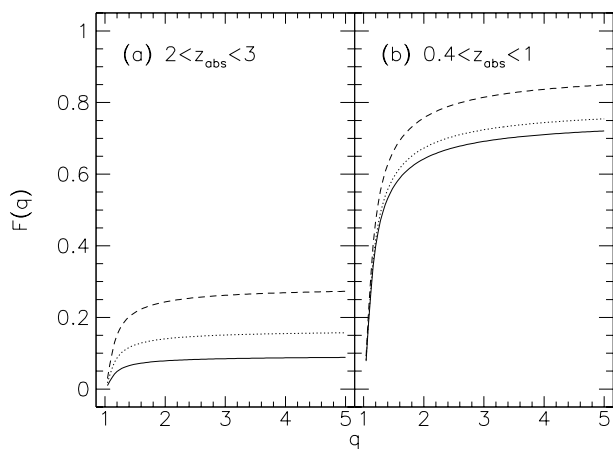


Figure 6.— The fraction of multiple images among bright QSOs ( $B \leq 16$ ) showing damped Ly $\alpha$  absorption with  $N \geq 10^{21} \text{ cm}^{-2}$  as a function of the maximum magnification ratio  $\mu_1/\mu_2 \leq q$  of their images. In panel (a) we consider absorbers with  $2 \leq z_{\text{abs}} \leq 3$ , while in panel (b),  $0.4 \leq z_{\text{abs}} \leq 1$ . In both panels,  $z_{\text{QSO}} = 3$ . The different line types describe the three cosmological models considered in figure 2.

Figure 6 shows the fraction of all QSOs which show damped Ly $\alpha$  absorption with  $N \geq 10^{21} \text{ cm}^{-2}$  that are multiply imaged with a magnification ratio of their images  $(\mu_1/\mu_2) \leq q$ . The two panels display results for different absorber-redshift intervals. For  $2 \leq z_{\text{abs}} \leq 3$ , the fraction of high column-density absorbers that show double images can be used as a sensitive test for the cosmological constant. For low-redshift absorbers ( $0.4 \leq z_{\text{abs}} \leq 1$ ), about 60%–80% of all QSOs should be doubly imaged with a magnification ratio below  $q = 2$ . The characteristic separation between the images is  $\sim 0.3''$  for an  $L_*$  spiral galaxy at  $z_{\text{abs}} \sim 1$ . Therefore, absorbers with  $N \geq 10^{21} \text{ cm}^{-2}$  can be used to flag possibly lensed quasars with small image separation. Since such absorbers are easy to identify through low-resolution spectroscopy, this approach can potentially enhance the efficiency of searches for new gravitational lenses with *HST* from its present value of  $\sim 1\%$  (Bahcall et al. 1992; Maoz et al. 1993) up to several tens of percent.

## 4. Conclusions

The signature of gravitational lensing is particularly strong for systems that are easy to observe, namely high column-density absorbers ( $N \gtrsim 10^{21} \text{ cm}^{-2}$ ) in the spectra of bright QSOs ( $B \lesssim 18$ ). There are five possibilities to verify the existence of lensing:

1. The apparent cosmological density of hydrogen should decline considerably towards low redshifts (cf. Fig. 3). Such a decline has, in fact, been observed (White et al. 1993;

Bahcall et al. 1993; Lanzetta et al. 1995). However, the interpretation of the observed trend in  $\Omega_{\text{HI}}(z)$  is ambiguous because it could also result from the consumption of gas by star formation (e.g., Kauffmann & Charlot 1994; Lanzetta et al. 1995). To avoid confusion with such evolutionary effects of the damped-Ly $\alpha$  absorber population, it is advantageous to make use of the dependences of the magnification bias on the source properties.

2. The inferred value of  $\Omega_{\text{HI}}$  should increase with increasing source luminosity (cf. Fig. 5) or source redshift (cf. Fig. 3) even if the absorber redshift interval is kept fixed. These effects cannot be imitated by an evolution of the population of damped-Ly $\alpha$  absorbers.
3. The column-density distribution for low-redshift absorbers in the spectra of high-redshift QSOs,  $f(N)$ , should show a pronounced peak followed by a sharp cut-off at high column-densities. For QSOs brighter than  $B \sim 17$  with redshifts  $z_{\text{QSO}} \gtrsim 2$ , and for non-evolving absorbers in the redshift interval  $z_{\text{abs}} \sim 0.4\text{--}1$ , the peak should appear around  $N \sim (3\text{--}5) \times 10^{21} \text{ cm}^{-2}$ . The location and height of the peak can be used to constrain the depth of the absorber potential wells or the value of the cosmological constant (cf. Fig. 2). Since  $\Omega_{\text{HI}}$  is obtained through an integral over the column density distribution of damped systems, the first two signatures listed above may be easier to probe than this third one. This could explain why the first signature may have already been observed.
4. When image splitting occurs, the absorption spectrum should show the superposition of two distinct absorption troughs corresponding to the different impact parameters of the two images. The two troughs are weighted by their corresponding image magnification factors (cf. Fig. 6). Since the equivalent width of each absorption feature scales as  $N^{1/2}$ , and since one of the images is usually faint, it may prove difficult to probe this spectroscopic signature.
5. High-resolution imaging of absorbers with deep potential wells may uncover the existence of multiple images. The image separation of  $\sim 0.3'' (v_c/220 \text{ km s}^{-1})^2$  expected for  $z_{\text{abs}} \sim 1$  is easily detectable with *HST* unless the magnification ratio of the images is extreme. The fraction of doubly imaged QSOs that show damped Ly $\alpha$  absorption with  $N \geq 10^{21} \text{ cm}^{-2}$  ranges between 10% for  $2 \leq z_{\text{abs}} \leq 3$  and 80% for  $0.4 \leq z_{\text{abs}} \leq 1$ . Therefore, strong damped Ly $\alpha$  systems may serve as reliable flags for lensed QSOs with small image splitting (cf. Fig. 6). The identification of such systems requires only low-resolution spectroscopy. The selection of bright QSOs which are known to have strong damped Ly $\alpha$  absorption lines may then be used to enhance the efficiency of searches for new gravitational lenses with *HST* (cf. Maoz et al. 1993).

As in any other astrophysical study, there are various factors that may complicate the analysis of observational data. First, obscuration by dust may hide the lensed images of a QSO. The abundance of dust in damped Ly $\alpha$  systems can be inferred from the reddening of the background QSOs. A comparison between the spectra of QSOs with and without damped Ly $\alpha$  systems implies that the most likely dust-to-gas ratio in damped Ly $\alpha$  systems at  $z_{\text{abs}} \gtrsim 2$  is only 5–20% of the Milky Way value (Fall et al. 1989; Pei et al. 1991; Fall & Pei 1993). Therefore, the high-redshift absorbers are expected to be optically thin for HI column densities  $\lesssim 10^{22} \text{ cm}^{-2}$ . Although the dust content of low-redshift absorbers could be higher than that, their obscuration is related to the low-extinction part of the

dust extinction curve in the V-band, where most QSO surveys are done. At low redshifts, the effect of dust can be readily corrected for by using the inferred obscuration profiles of nearby disk galaxies (e.g., Byun 1993; Byun et al. 1994; Jansen et al. 1994; Rix 1994).

Note that the bending of light rays from the source due to lensing tends to weaken the effect of dust as it provides a minimum impact parameter, of order  $\sim 1$ -2 kpc, for the bright image of the QSO. Thus, if dust obscuration is strong in the inner part of damped Ly $\alpha$  absorbers, then the significance of lensing may be emphasized even more, because without lensing fewer QSOs would have been seen behind the center of the absorber. Aside from adding QSOs through the magnification bias, the ray-bending due to lensing brings additional QSOs into view that would otherwise be hidden behind a thicker layer of dust.

A second complication to our analysis involves possible clumpiness of the HI distribution in the absorbers. Clumpiness would tend to broaden the distribution of column densities at a given impact parameter beyond the geometric spread induced by different inclinations. This effect would then broaden the peaks shown in figure 2. An argument against the existence of strong ( $\gtrsim 30\%$ ) clumpiness on small scales ( $\lesssim 1$ -2 kpc) is provided by the similarity between the column densities observed in the two images of the lensed QSO 0957+561 at  $z_{\text{QSO}} = 1.41$ ; the separate lines of sight corresponding to the two images cross a common damped Ly $\alpha$  absorber at  $z_{\text{abs}} = 1.391$  and show a similar column density in their spectra (Turnshek & Bohlin 1993). In general, the higher the overdensity of the HI clumps, the smaller is their cross-section and the less likely they are to appear in absorption spectra. Clumpiness should be less important for estimates of averaged quantities such as  $\Omega_{\text{HI}}$  than for differential quantities like  $f(N)$ .

Finally, a third complication to our modeling may arise from possible evolution in the properties of the absorbers. If the observed HI disks are much bigger at high redshift, then for a given HI column density the characteristic impact parameter increases and the lensing signatures are weakened relative to our no-evolution model. However, it should be easy to disentangle the pure lensing effect from any such evolutionary effect by examining the second signature mentioned above.

Recently, there has been considerable interest in the cosmological abundance of damped Ly $\alpha$  systems as a means of constraining variants of cold dark matter cosmologies, such as the mixed dark-matter (MDM) model, in which galaxies form relatively late (Kauffmann & Charlot 1994; Ma & Bertschinger 1994; Mo & Miralda-Escudé 1994). The magnification bias derived in this paper should in general be incorporated into those studies. In addition, the observed sample of absorbers may be biased towards higher velocity dispersion  $\sigma_v$  because the magnification bias depends strongly on  $\sigma_v$ . However, this effect is limited by the exponential cut-off of the Schechter luminosity function.

Some of the gravitational-lensing signatures listed above were not discovered observationally in the past due to an unfortunate combination of selection effects. Ground-based observations were limited to absorbers at high redshift, while *IUE* observations (Lanzetta et al. 1995) focused on low redshift sources. In both cases the signature of lensing was artificially minimized by the lensing geometry. Forthcoming observations with *HST* could easily detect a few of the above five signatures if properly designed. The search strategy should focus on finding high column-density ( $N \gtrsim 10^{21} \text{ cm}^{-2}$ ) absorbers in the spectra of

bright ( $B \lesssim 16-17$ ), high-redshift ( $z_{\text{QSO}} \gtrsim 2-3$ ) QSOs. Detection of the peaks shown in figure 2 or the fraction of multiply imaged QSOs shown in figure 6 may be possible in a sample of more than ten damped Ly $\alpha$  systems with  $N \gtrsim 10^{21} \text{ cm}^{-2}$  and  $0.5 \lesssim z_{\text{abs}} \lesssim 1$ . Quantitative measurement of these and the other lensing signatures can be used to constrain the gravitational-potential depth of the absorbers and the cosmological constant.

*Acknowledgements.* We thank Emilio Falco for useful comments. MB was supported in part by the Sonderforschungsbereich SFB 375-95 of the Deutsche Forschungsgemeinschaft.

## References

- Aaronson, M., Huchra, J., & Mould, J. 1979, *ApJ*, 229, 1  
 Bahcall, J. N., & Peebles, P. J. E. 1969, *ApJ*, 156, L7  
 Bahcall, J. N., Maoz, D., Schneider, D. P., Yanny, B., & Doxsey, R. 1992, *ApJ*, 392, L1  
 Bahcall, J. N., et al. 1993, *ApJS*, 87, 1  
 Boyle, B. J., Shanks, T., & Peterson, B. A., 1988, *MNRAS*, 235, 935  
 Briggs, F. H., Wolfe, A. M., Liszt, H. S., Davis, M. M., & Turner, K. L. 1989, *ApJ*, 341, 650  
 Broeils, A. H., van Woerden, H., 1994, *A&AS*, 107, 129  
 Burbidge, G., Odell, S. L., Roberts, D. H., & Smith, H. E., 1977, *ApJ*, 218, 33  
 Byun, Y. I. 1993, *PASP*, 105, 993  
 Byun, Y. I., Freeman, K. C., & Kylafis, N. D. 1994, *ApJ*, 432, 114  
 Davies, J. I., Phillipps, S., Boyce, P. J., & Disney, M. J. 1993, *MNRAS*, 260, 491  
 Fall, S. M., & Pei, Y. C. 1993, *ApJ*, 402, 479  
 Fall, S. M., Pei, Y. C., & McMahon, R. G. 1989, *ApJ*, 341, L5  
 Hartwick, F. D. A., & Schade, D., 1990, *ARA&A*, 28, 437  
 Holmberg, E. B. 1975, in: *Galaxies and the Universe*, eds. A. Sandage, M. Sandage, & J. Kristian (Chicago: University Press), p. 151  
 Jansen, R. A., Knapen, J. H., Beckman, J. E., Peletier, R. F., & Hes, R. 1994, *MNRAS*, 270, 373  
 Kauffmann, G., & Charlot, S. 1994, *ApJL*, 430, L97  
 Kochanek, C. S. 1991, *ApJ*, 373, 354  
 Kochanek, C. S. 1992, *ApJ*, 384, 1  
 Kronberg, P. P., Perry, J. J., & Zukowski, E. L. H. 1992, *ApJ*, 387, 528  
 Lanzetta, K. M., & Bowen, D. V. 1992, *ApJ*, 391, 48  
 Lanzetta, K. M., Wolfe, A. M., Turnshek, D. A., Lu, L., McMahon, R. G., & Hazard, C. 1991, *ApJS*, 77, 1  
 Lanzetta, K. M., Wolfe, A. M., & Turnshek, D. A. 1995, *ApJ*, 440, 435  
 Lu, L., & Wolfe, A. M. 1994, *AJ*, 108, 44  
 Lu, L., Wolfe, A. M., Turnshek, D. A., & Lanzetta, K. M., 1993, *ApJS*, 84, 1  
 Ma, C.-P., & Bertschinger, E. 1994, *ApJL*, 434, L5  
 Maoz, D., et al. 1993, *ApJ*, 409, 28  
 Marzke, R. O., Geller, M. J., Huchra, J. P., & Corwin Jr., H. G. 1994, *AJ*, 108, 437  
 Mo, H. J., & Miralda-Escudé, J. 1994, *ApJL*, 430, L25  
 Narayan, R., & Wallington, S., 1993, in: *Gravitational Lenses in the Universe*, Proc. 31st Liège Astrophys. Coll., eds. J. Surdej et al.  
 Peebles, P. J. E., 1993, *Principles of Physical Cosmology* (Princeton: University Press)  
 Pei, Y. C., 1995, *ApJ*, 438, 623  
 Pei, Y. C., Fall, S. M., & Bechtold, J. 1991, *ApJ*, 378, 6  
 Perry, J. J., Watson, A. M., Kronberg, P. P. 1993, *ApJ*, 406, 407  
 Peterson, B. M., Strom, S. E., & Strom, K. M., 1979, *AJ*, 84, 735  
 Pettini, M., Smith, L. J., Hunstead, R. W., & King, D. L. 1994, *ApJ*, 426, 79  
 Rix, H.-W. 1994, to appear in Proc. on the Opacity of Spiral Disks, NATO Advanced Research Workshop, (Cardiff, July 1994), ed. J. Davies, IAS preprint 94/61  
 Rix, H.-W., Schneider, D. P., & Bahcall, J. N. 1992, *AJ*, 104, 959

- Schneider, P., 1992, *A&A*, 254, 14
- Schneider, P., Ehlers, J., & Falco, E. E., 1992, *Gravitational Lenses* (Heidelberg: Springer)
- Schechter, P., 1976, *ApJ*, 203, 297
- Steidel, C. C., Pettini, M., Dickinson, M., & Persson, S. E. 1994, *AJ*, 108, 2046
- Steidel, C. C., Bowen, D. V., Blades, J. C., & Dickinson, M. 1995, *ApJL*, 440, L45
- Strauss, M. A., & Willick, J. A., 1995, *Physics Reports*, in press
- Thomas, P. A., & Webster, R. L. 1990, *ApJ*, 349, 437
- Tóth, G., & Ostriker, J. P. 1992, *ApJ*, 389, 5
- Tully, R. B., & Fisher, J. R., 1977, *A&A*, 54, 661
- Turner, E. L. 1990, *ApJL*, 365, L43
- Turnshek, D. A., & Bohlin, R. C. 1993, *ApJ*, 407, 60
- Turnshek, D. A., Wolfe, A. M., Lanzetta, K. M., Briggs, F. H., Cohen, R. D., Foltz, C. B., Smith, H. E., & Wilkes, B. J. 1989, *ApJ*, 344, 567
- Tytler, D. 1987, *ApJ*, 321, 49
- Welter, G. L., Perry, J. J., & Kronberg, P. P. 1984, *ApJ*, 279, 19
- White, R. L., Kinney, A. L., & Becker, R. H. 1993, *ApJ*, 407, 456
- Wolfe, A. M. 1988, in *QSO Absorption Lines: Probing the Universe*, ed. J. C. Blades, D. A. Turnshek, & C. A. Norman (Cambridge: University Press), p. 297
- Wolfe, A. M., Lanzetta, K. M., & Oren, A. L. 1992 *ApJ*, 388, 17
- Wolfe, A. M., Turnshek, D. A., Smith, H. E., & Cohen, R. D., 1986, *ApJS*, 61, 249
- Wolfe, A. M., Turnshek, D. A., Lanzetta, K. M., & Lu, L. 1992, *ApJ*, 404, 480
- Wolfe, A. M., Turnshek, D. A., Lanzetta, K. M., & Oke, J. B. 1992, *ApJ*, 385, 151
- Zaritsky, D. 1995, *ApJL*, in press